CALCULATION MODEL FOR THERMO-MECHANICAL COUPLING AND 3D NUMERICAL SIMULATION FOR CONCRETE TOWER OF CABLE-STAYED BRIDGE

Jun Song[1*] and Fuyan Chen[2]

*[1] School of Civil Engineering, Ludong University, Yantai, Shandong, China;
[2]School of Civil Engineering, Ludong University, Yantai, Shandong, China.

Email: songjun198298@163.com

ABSTRACT

Heat transfer theory for concrete tower of cable-stayed bridge will be the basis of the temperature field analysis using the finite element method analysis of the stress field of indirect coupling, accurate analysis of the internal structure of the transient temperature and stress field stacked Jiahousuota stress distribution. In real bridge, for example, solving the temperature stress on the tower, and demonstrated: Solving transient temperature field finite element method can accurately simulate the temperature distribution in Sarasota; the treatment temperature change methods - mechanical coupling problem, can temperature load and other effective combination of load stress field, resulting in accurate stress distribution in the structure.

Keywords: Temperature, Mechanical properties, Thermo-mechanical coupling, Cable-stayed bridge.

1. INTRODUCTION

Due to poor heat conduction properties of concrete, its surroundings and solar radiation temperature changes and other factors, to the surface rapidly warming or cooling, heat transfer inside the concrete needs a long time to reach equilibrium, while the concrete structure surface continuous with the surrounding environment to carry out heat exchange, so the concrete structure temperature field and the temporal changes over time showed significant non-linear distribution. Nonlinear transient temperature distribution in the cross section of the field will produce not only displacement, stress and temperature constraints and a large temperature stress from restraint, which appear temperature and stress field coupling effect on the structural discontinuity lee.

Temperature has a great influence on the mechanical properties of concrete, temperature coupled stress fracture behavior occasion of concrete, mainly fracture toughness and fracture energy, attracting the attention of many researchers. Prokopski by testing analysis and comparison of changes in ordinary concrete and refractory concrete fracture toughness in the range of 20 ℃ -1100 ℃, found two concrete fracture toughness are reduced with increasing temperature. Nielsen et al., Respectively, and Menou by experimental analysis of concrete-like material fracture energy, tensile strength and other parameters vary with temperature, that the rough fracture surface is the main cause of the fracture energy varies with temperature. But now a lot of research results were from tests.

2. CALCULATION MODEL FOR THERMO-MECHANICAL COUPLING

As we all know, poor thermal conductivity is a disadvantage of concrete materials [1] ~ [11], temperature changes caused by solar radiation easily to the surface rapidly heating and cooling, concrete internal equilibrium heat transfer the basic needs of a very long period, while Concrete needs heat exchange with the environment, and therefore the temperature field in concrete structure over time and is nonlinear transient changes in distribution. - Section nonlinear transient temperature distribution will not only displaced, but also have a greater self-restraint stress and temperature constraint stress, which appears temperature and stress field coupling effect on the force structure is extremely unfavorable. Temperature changes have a significant impact on its mechanical properties, temperature field and stress field coupling will accelerate cracked concrete, mainly in the fracture energy and fracture toughness. Prokop ski [11]~[14]experimentally analyzed the changes in ordinary concrete and refractory concrete fracture toughness, fracture toughness were found to increase with increasing temperature but will decrease. Nielsen and Menu [15]~ [20]and other binding assay analyzes the tensile strength and fracture energy of concrete with changes in temperature, they think rough fracture surface is the main cause of the fracture energy varies with temperature, is obtained according to the heat conduction equation node heat rate vector, and then introduced as a load stress field solving equations, formulas such as (1) as follows:

$$\{K\}\{U\} = \{F^R\} + \{F^A\} \qquad (1)$$

$\{K\}$ stands fortotal stiffness matrix, $\{U\}$ is nodal displacements matrix; $\{F^R\}$ is reaction force vector.

$$\{F^A\} = \{F^{nd}\} + \{F^{ac}\} + \sum_{m=1}^{N}\left(\{F^{th}\} + \{F^{pr}\}\right) \qquad (2)$$

$\{F^{nd}\}$ stands for he force on the node, $\{F^{ac}\}$ is acceleration vector, $\{F^{th}\}$ is thermal unit vector, $\{F^{pr}\}$ is pressure unit vector.

$\{F_e^{th}\} = \int_{vol}[B]^T[D]\{\varepsilon\}^{th}d(vol)$, $[B]$ stands for strain - displacement matrix, $\{\varepsilon\}^{th}$ is thermal strain matrix, vol is volume [147]. When the heat conduction equation and the stress field of Combined Solution of achieving two field coupling process, we have tower temperature stress distribution.

3. CABLE-TEMPERATURE FIELD AND TEMPERATURE FIELD COUPLED STRESS CALCULATION

3.1 Temperature field calculation

Temperature field boundary conditions include external borders and internal boundaries, the former mainly by solar radiation, which is mainly radiant heat exchange, concrete pylon outside the boundary at any instant, the heat flow to follow the following equation

$$-\lambda\partial\theta/\partial n = q_s q_c q_l \qquad (3)$$

In formula, q_s is solar radiation energy, $q_s = a_s \bullet I$, a_s is blackness coefficient, q_c is convective heat exchange; q_l is

radiation heat transfer, $q_l = \sigma e\left[(T+273)^4 - (T_a+273)^4\right]$, σ =5.676x10⁻⁸ W /m² K⁴,e is 0.88,Assume that radiation heat transfer coefficient

$$\beta_\gamma = \sigma e\left[(T+273)^2 + (T_a+273)^2\right](T+T_a+2\times273), \quad (4)$$

Then it can express

$$-\lambda\partial T/\partial n = -a_s I + \beta_c(T-T_a) + \beta_\gamma(T-T_a). \qquad (5)$$

Hypothesis $\beta = \beta_c \beta_\gamma$,Combined heat conduction equation

$$T_a' = T_a + a_s I/\beta \qquad (6)$$

$I = I_a + I_d$, I_a is the intensity of the sun's radiation, I_d is scattering intensity.

Atmospheric temperature

$$T_a(t) = (T_{a\max} + T_{a\min})/2 + \sin\left[(t-9)\pi/12\right](T_{a\max} - T_{a\min})/2$$

Formula to solve, $T_{a\max}$, $T_{a\min}$ is the maximum daily temperature and minimum daily temperatures. Temperature boundary conditions within the boundary of tower:

$$\lambda\partial T/\partial n + \beta_\gamma(T-T_a) + q_s = 0 \qquad (7)$$

$\beta_\gamma(T-T_a)$ is convective heat exchange, T_a is inside temperature,The average of the measured values of available alternatives, can also be determined empirically. Therefore, the temperature inside the tower can be expressed by the following boundaries formula:

$$T_a' = T_a - q_s/\beta_c \qquad (8)$$

β_c Considers wind conditions,is 5.7W / m2 ℃ ; q_s is radiation Heat Transfer. When radiation heat q_s transfer requires the solution of two surfaces in between tower demand angle factor F_{ij},The calculation method may be hidden.
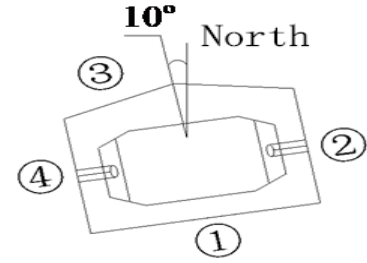

Figure 1. Orientation of tower

Bradenton is located orientation pylon four faces at different times of the day different sunshine effect shown in Figure.1. Morning ①, ② two side subject to solar radiation, mainly as heating ② surface; afternoon ③, ④ affected both sides of the sun, ④ surface influenced by solar radiation. Figure.2 for the tower at 13:00 am the temperature field contours.
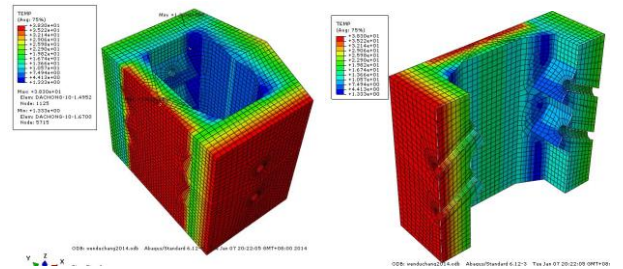

Figure 2. Temperature distribution

3.2 Temperature stress calculation

Without considering the impact of stress singularity at constant normal stress loads (dead weight + cable force) around the hole Sarasota X direction is 1.537Mpa, positive stress Y direction is 1.14Mpa, the normal stress X direction is 1.02Mpa .
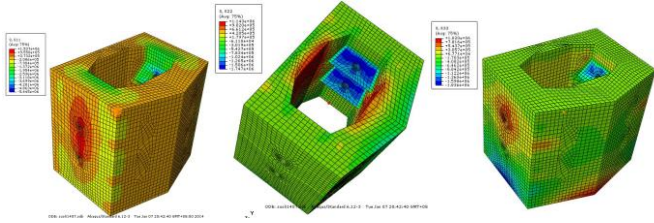
Figure 3. Stress contours

In order to accurately calculate the temperature - stress field coupling, the calculated transient temperature distribution along the tower wall thickness distribution of the maximum temperature difference of temperature distribution and empirical formulas were used as temperature load is coupled to the solid model to solve the stress distribution in the temperature stress calculation, obtained by calculating the maximum temperature stress and dead loads (gravity loads and cable tension) is a linear superposition of the stress field, to get the actual structure of the stress distribution, as shown in Figure.3 ~ Figure.6. Then superimposed with constant load on the pylon maximum transverse tensile stress is 2.038MPa.
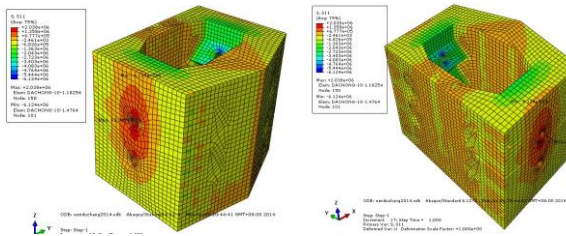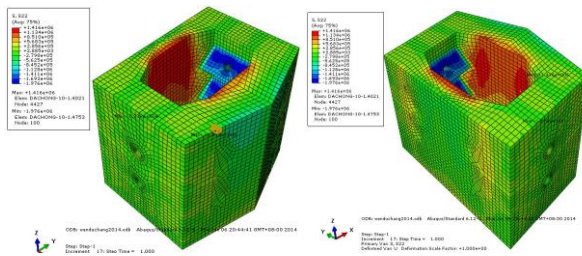

Figure 4. X direction normal stress

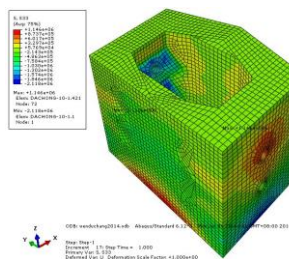

Figure 5. Y direction normal stress

Figure 6. Z direction normal stress

From the above analysis we can get this conclusion:

(1) According to the distribution of temperature stress Tower, using the transient temperature field-coupled stress to analyze the stress distribution under the tower of the stress state capable of precise reaction tower in a real environment subject to various loads structures.

(2) Through heat conduction equation, combined with Abaqus temperature distribution structure to analyze, calculate numerical example can be seen in comparison with the experimental results using thermal conductivity-Transient effects of temperature and the temperature difference between the results of the finite element method coupling calculation can be a true reflection of Bradenton.

4. CONCLUSIONS

This chapter introduces the overall form structure support projects in Guangxi big red bridge, by Madis Civil calculate the maximum cable tension cable-stayed bridge in various combinations during the operational phase, and then combined with ABAQUS and FRANC3D tower segments were local Finite element analysis of crack propagation and calculates the relationship between the stress intensity factor and the tower surface fractal dimension and load between the final analysis Sarasota temperature field - mechanical properties under stress field coupling tower, the main conclusions are as follows:

(1) Fractal theory using the finite element means under conditions different levels of load calculation and analysis of the pylon, finite element results tables around the outside of the cable guide hole tower prone to tensile stress concentration phenomenon and led to cracks, damage and failure Bradenton It is actually a process of increasing dimension, the fractal dimension of the larger tower higher level of security, the higher the risk, so you can use the fractal dimension theory carve tall tower of safety evaluation.

(2) According to the distribution tower temperature stress using transient temperature field - coupled stress analysis stress method tower, the stress distribution under a reaction tower capable of accurately in a real environment by various load structure; and by heat conduction equation, combined with Abaqus temperature distribution structure is analyzed, for example, calculated and measured results can be seen as relatively thermal conductivity - coupling calculation results of FEM can be a true reflection of the Tower of transient temperature field and the temperature difference between the effects.

REFERENCES

1. Sang-Hoon Kim, Jung-Ju Lee and Il-Bum Kwon, Monitoring of Beam Deflection Subjected to Bending Load Using Brillouin Distributed Optical Fiber Sensors, *Proceedings of SPIE-The International Society for Optical Engineering*, 2001: 63-69. DOI: 10.1117/12.435543.

2. Chai, J., Wei, S. M., Chang, X. T., Liu, J. X., Monitoring Deformation and Damage on Rock Structures with Distributed Fiber Optical Sensing [J], *International Journal of Rock Mechanics and Mining Sciences*, 2004, 41(5): 1-6. DOI: 10.1016/j.ijrmms.2003.12.008.

3. Ou Jinping, Hou Shuang, Seismic Damage Identification Using Multi-Line Distributed Fiber Optic Sensor System, *Proceedings of SPIE*, 2005: 1003-1008. DOI: 10.1117/12.612449.

4. Roger G. Duncan, Brooks A. Childers, Dawn K. Gifford, Don E. Pettit, Andrew W. Hickson, Timothy L. Brown, Distributed Sensing Technique for Test Article Damage Detection and Monitoring, *Proceedings of SPIE*[C], 2003: 367-375.5.

5. S. L. Soo, Boundary Layer Motion of a Gas-Solid Suspension, *Proc. Symp. Interaction between Fluids and Particles*, vol. 1, pp. 50-63, 1962.

6. W. B. Thompson, Kinetic Theory of Plasma, *M. N. Rosenbluth (ed.), Advanced Plasma Theory*, chap. 1, Academic Press, New York, 1964.

7. F. Bakhtiari-Nejad, A. Khorram, M. Rezaeian. Analytical Estimation of Natural Frequencies and Mode Shapes of a Beam Having Two Cracks, *International Journal of Mechanical Sciences*, 2014:193–202. DOI: 10.1016/j.ijmecsci.2013.10.007.

8. Zhe Cheng, Niaoqing Hun, Xiaofei Zhang, Crack Level Estimation Approach for Planetary Gearbox Based On Simulation Signal and GRA, *Journal of Sound and Vibration*, 2012: 5853–5863. DOI: 10.1016/j.jsv.2012.07.035.

9. Mohammad H. F. Dado, Omar A. Shpli, Crack Parameter Estimation in Structures Using Finite Element Modeling, *International Journal of Solids and Structures*, 2003: 5389–5406.

10. Ahmed A. Elshafey, Nabil Dawood, H. Marzouk, M. Haddara, Crack Width in Concrete Using Artificial Neural Networks, *Engineering Structures*, 2013:676–686. DOI: 10.1016/j.engstruct.2013.03.020.

11. Masayuki Kamaya, Estimation of Elastic-Plastic Fracture Toughness by Numerical Simulation Based on a Stress-Based Criterion for Ductile Crack Initiation, *International Journal of Pressure Vessels and Piping*, 2013: 1-7.

12. Martin Noel, Khaled Soudki, Estimation of the Crack Width and Deformation of FRP-Reinforced Concrete Flexural Members with and without Transverse Shear Reinforcement, *Engineering Structures* 2014: 393–398.

13. Minhhuy Le, Jinyi Lee, Jongwoo Jun, Jungmin Kim, Estimation of Sizes of Cracks on Pipes in Nuclear Power Plants Using Dipole Moment and Finite Element Methods, *NDT&E International*, 2013: 56–63.

14. Gang Li, Shuanhai He, Yongfeng Ju, Kai Du, Long-Distance Precision Inspection Method for Bridge Cracks with Image Processing, *Automation in Construction*, 2013. DOI: 10.1016/j.autcon.2013.10.021.

15. Ahmed A. Elshafey, Nabil Dawood, H. Marzouk, M. Haddara, Predicting of Crack Spacing for Concrete by Using Neural Networks, *Engineering Failure Analysis* 2013, 31:344–359. DOI: 10.1016/j.engfailanal.2013.02.011.

16. J. H. Espina-Herna´ndez, E.Ramrez-Pacheco, Rapid Estimation of Artificial Near-Side Crack Dimensions in Aluminium Using a GMR-Based Eddy Current Sensor, *NDT&E International*, 2012, 51: 94–100.

17. M. Hadj Meliani, Z. Azari, G. Pluvinage, Yu. G. Matvienko, The Effective T-Stress Estimation and Crack Paths Emanating from U-Notches, *Engineering Fracture Mechanics*, 2010. 77:1682–1692. DOI: 10.1016/j.engfracmech.2010.03.010.

18. Ahmed A. Elshafey, Nabil Dawood, Crack Width in Concrete Using Artificial Neural Networks, *Engineering Structures*, 2013, 52: 676–686. DOI: 10.1016/j.engstruct.2013.03.020.

19. Ahmed A. Elshafey. Nabil Dawood. Predicting of crack spacing for concrete by using neural networks, *Engineering Failure Analysis*, 2013, 31: 344–359. DOI: 10.1016/j.engfailanal.2013.02.011.

20. K. G. Papakonstantinou, M. Shinozuka, Probabilistic. Model for Steel Corrosion in Reinforced Concrete Structures of Large Dimensions Considering Crack Effects, *Engineering Structures*, 2013, 57: 306–326. DOI: 10.1016/j.engstruct.2013.06.038.

21. Martin Noël, Khaled Soudki, Estimation of the Crack Width and Deformation of FRP-Reinforced Concrete Flexural Members with and without Transverse Shear Reinforcement, *Engineering Structures*, 2014, 59:393–398.